Lawrence Berkeley National Laboratory

Title
Release of impurities from structural defects in polycrystalline silicon solar cells

Permalink
https://escholarship.org/uc/item/6zw456d5

Author
Mchugo, S.A.

Publication Date
1997-04-04

ERNEST ORLANDO LAWRENCE
BERKELEY NATIONAL LABORATORY

Release of Impurities from Structural Defects in Polycrystalline Silicon Solar Cells

S.A. McHugo and M. Imaizumi
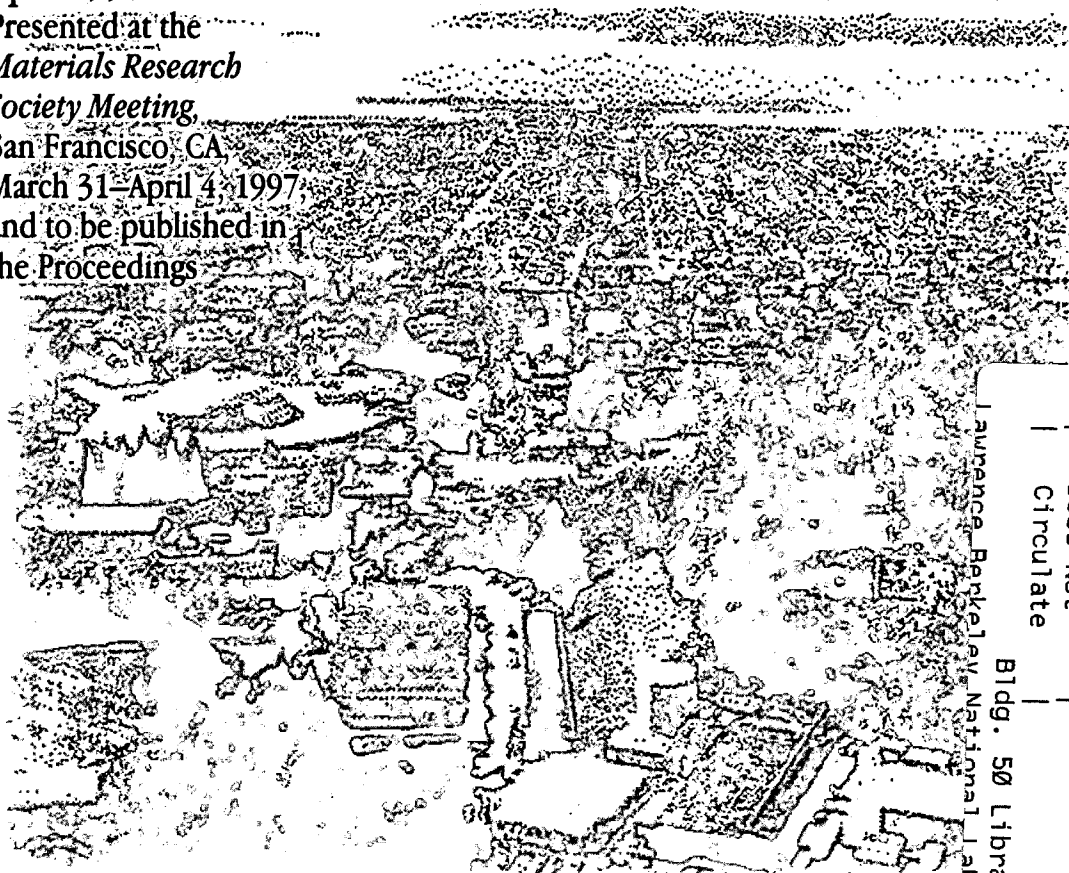
Accelerator and Fusion Research Division

DISCLAIMER

RELEASE OF IMPURITIES FROM STRUCTURAL DEFECTS IN POLYCRYSTALLINE SILICON SOLAR CELLS*

S.A. McHugo[1], M. Imaizumi[2]

[1]Advanced Light Source
Accelerator & Fusion Research Division
Ernest Orlando Lawrence Berkeley National Laboratory
University of California, Berkeley, California 94720

[2]Toyota Technological Institute
Nagoya 468
Japan

RELEASE OF IMPURITIES FROM STRUCTURAL DEFECTS IN POLYCRYSTALLINE SILICON SOLAR CELLS

S.A. McHugo* and M. Imaizumi**

* Lawrence Berkeley National Laboratory, Advanced Light Source, Berkeley, CA 94720, USA

**Toyota Technological Institute, Nagoya 468, JAPAN

ABSTRACT

It is critical to understand the behavior of metallic impurities in polycrystalline silicon used for solar cells. These impurities significantly increase the minority carrier recombination rate and, in turn, degrade cell performance. Impurity gettering is a commonly used method to remove these impurities from the material, however, past work has suggested that impurity release from structural defects drastically limits the gettering process. Presently, there is only a limited understanding of impurity release from structural defects. In this work, a correlation between structural defects and the location of metal impurities in as-grown material is established and the release of nickel and copper from structural defects in polycrystalline silicon was studied in as-grown material and after sequential thermal treatments which dissolve the impurities into the silicon matrix. Synchrotron-based x-ray fluorescence impurity mapping with spatial resolution of ≈1μm, was used to determine impurity distributions after each thermal treatment.

INTRODUCTION

Polycrystalline silicon is a very interesting material for terrestrial solar cells. Its low cost and respectable energy conversion efficiency (12-15%) makes it arguably the most cost competitive material for large-volume solar power generation. However, the solar cell efficiency of this material is severely degraded by regions of low minority carrier diffusion length which have been shown to possess both dislocations and microdefects. These structural defects are known to decrease diffusion length values with intentional transition metal decoration introduction [1-6]. Therefore, gettering of metal impurities from the material would be expected to greatly enhance solar cell performance. Contrary to this rationale, experiments using frontside phosphorus and/or backside aluminum treatments have been found to improve regions with high diffusion lengths while having little or no effect on the low diffusion length regions and in turn only slightly improving the overall cell performance [7-11]. Recent work has suggested metal impurity release from structural defects is the rate limiting step for gettering [11,12] in polysilicon. The goal of this research is to correlate the locations of metal impurities with structural defects in as-grown polycrystalline silicon and to study the kinetics of metal impurity release from these defects during thermal processing.

EXPERIMENT

We have performed studies on polycrystalline solar cell silicon (polysilicon) in the as-grown state, after rapid thermal annealing and following an aluminum gettering treatment. The polysilicon is boron doped with a resistivity of 0.8-1.5 ohm-cm and has an oxygen concentration of $1-2x10^{17}$ atoms/cm^3. The wafers were formed by a casting method with subsequent cutting and etching ($HNO_3+H_2O_2$) to remove the damaged surface layer. With Surface Photovoltage (SPV) measurements, the minority carrier diffusion length was measured over a 10 x 10cm polysilicon wafer in the as-grown material. Regions of the material were removed by use of a wafer dicing saw. All samples were cleaned with VLSI grade pirahna (H_2SO_4:H_2O_2) and HF dips prior to anneals as well as SPV and XRF measurements. Low diffusion length regions were rapid thermal

annealed at 500°C for 30 seconds with a rapid quench to room temperature ($\approx$1000K/s). This was followed by an aluminum gettering treatment at 800°C for 3 hours using a 1μm aluminum layer on the sample backside. The frontside of the samples were analyzed using synchrotron-based x-ray fluorescence (xrf) mapping at the Advanced Light Source in order to determine metal impurity content and distribution at each step of the sample processing: in the as-grown state, following the 500°C annealing and finally after the 800°C aluminum gettering treatment. The xrf equipment uses 12.4keV monochromatic radiation to excite elements in the sample with a spatial resolution of 1x1μm and a Si:Li detector to measure fluorescence x-rays from the sample, all in atmospheric conditions. With this configuration, the apparatus is capable of detecting trace concentrations of elements with z > 13. Sensitivities are element specific but, for example, the system can detect Ni or Cu precipitates/agglomerates in silicon greater in size than 2-5nm. The sampling depth for metal impurities in silicon is on the order of 50μm. Impurity concentrations are quantified with the use of standard samples of known impurity levels. The impurity mapping was performed on the same regions after each processing step in order to track the dissolution of metal impurity precipitates. Etch features on the sample surface, caused by slight preferential etching of grain boundaries during the $HNO_3+H_2O_2$ etch which removed the damaged layer, were used as reference points to re-locate areas of interest for xrf measurements after each processing step. Following aluminum gettering and xrf analysis, the diffusion length was measured with SPV and the samples were preferentially etched with a Wright-Jenkins [13] etch to reveal etch pits associated with structural defects. A scanning electron microscope was used in secondary mode to image these pits. From these images and the xrf maps, a correlation between structural defects and metal impurity distribution was exactly identified.

RESULTS

The diffusion length mapping of the polysilicon wafer indicated the material has wide ranging values of minority carrier diffusion length, from <10μm to $\approx$80μm. A low diffusion length region of 10μm was selected from the wafer and analyzed with xrf mapping. Maps of the as-grown Ni and Cu distributions are shown in Figures 1a&b. The impurities are located at the
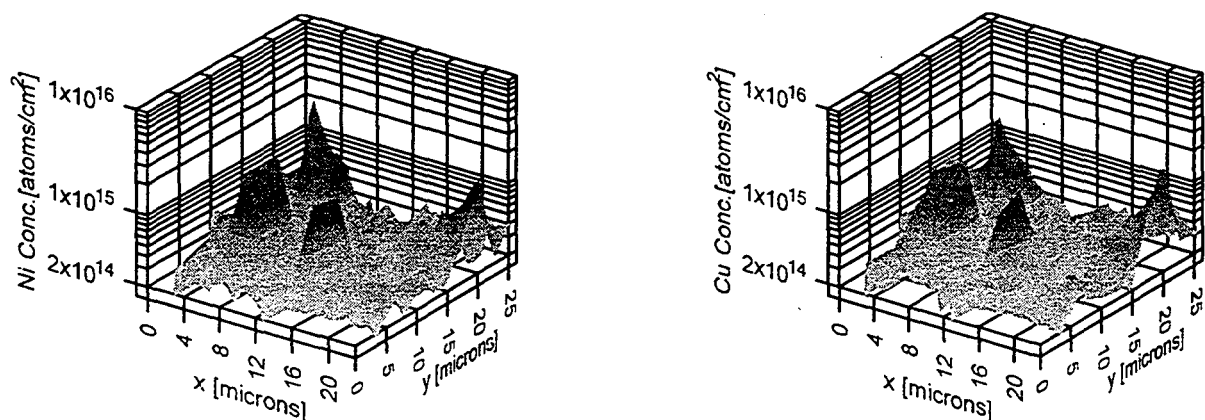
Figures 1a&b: Ni and Cu distributions in as-grown polycrystalline silicon. Note the discrete agglomerations of impurities.

same positions with sizes of 2-5μm. These may be single precipitates or clusters of smaller precipitates. It is interesting to note the impurities are located at exactly the same positions, suggesting these sites are the preferred precipitation site during the slow cool from growth and possibly that the Cu is alloyed with Ni. The same sample was annealed at 500°C for 30 seconds

with a rapid quench to room temperature in order to freeze in the kinetics of impurity dissolution. Based on diffusion data of Ni and Cu in silicon, [14], one would expect significant diffusion of the both impurities for this anneal temperature and time. Following this anneal we have scanned the same region as in Figure 1 using the x-ray fluorescence microprobe. These results are shown in Figures 2a&b. Most impurity agglomerations have been dissolved.
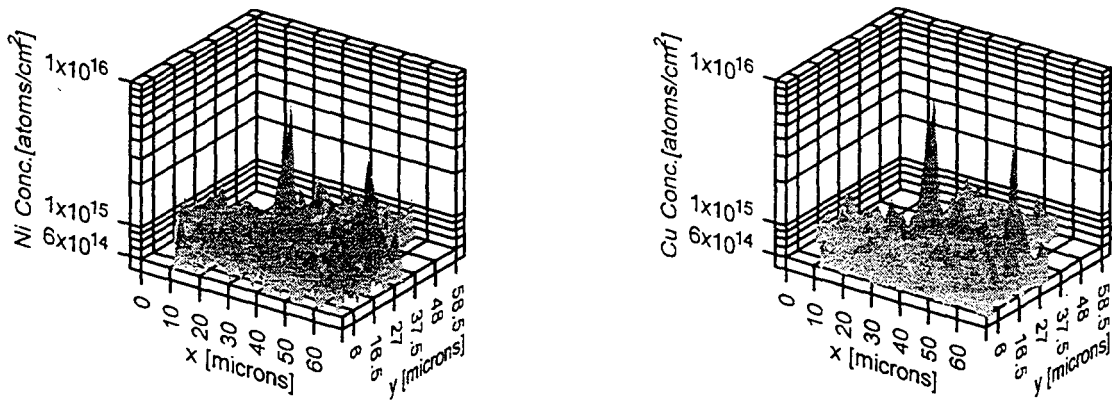

Figure 2a&b: Ni and Cu distributions in polycrystalline silicon after a 500°C-30 sec RTA quench. Note only certain discrete agglomerations of impurities have remained from the as-grown state (Figure1).

The few remaining points with Ni and Cu correlate with peaks in Figures 1a&b at y=22.5µm. Again both impurities are present in the same location. They are no greater in size than 1 µm, the spatial resolution of the xrf system. The initial size of the Ni and Cu precipitates can be approximated based on this data and with theoretical models of precipitate dissolution which consider the dissolution process to be limited by impurity diffusion from the precipitate[15,16]. From these models it is calculated that Ni precipitates with a radii of <3nm and a Cu precipitates with a radii of <10nm will dissolve in 30sec at 500°C. This high dissolution rate is primarily due to the high diffusivity and solubility of these impurities in silicon. This theoretical modeling taken in conjuction with the size of the Ni and Cu rich regions in Figures 1&2, suggests most of the as-grown impurities are in the form of small precipitates which are clustered over micron-scale regions of the material. The few impurity rich points remaining after the dissolution treatment are greater in size than ≈10nm but are no greater than the xrf spatial resolution (1µm).

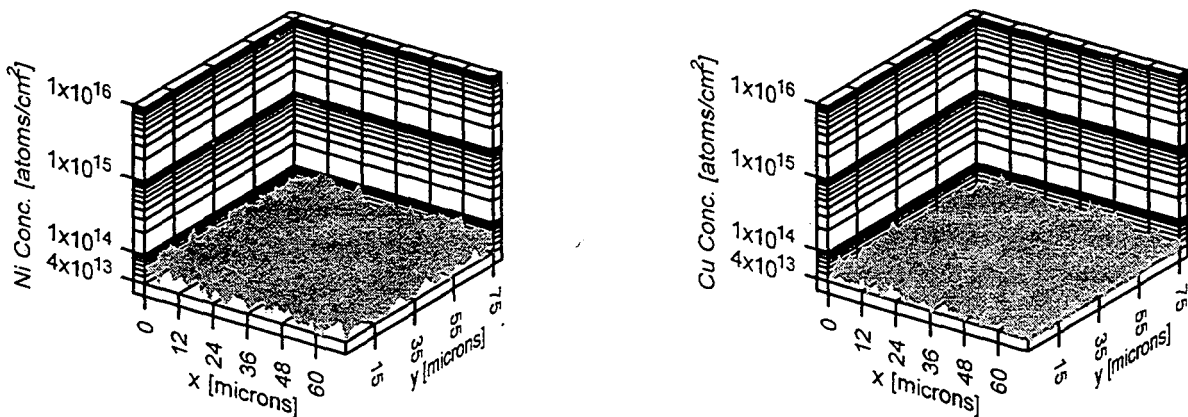The same sample was aluminum gettered for 3 hours at 800°C and the same regions as in

Figure 3a&b: Ni and Cu distributions in polycrystalline silicon after a 800°C-3 hr aluminum gettering treatment. All previous impurity agglomerations have been dissolved to a size at least smaller than the sensitivity of the system (2-5nm).

Figures 1&2 were analyzed with xrf mapping, the results are shown in Figures 3a&b. No Cu or Ni agglomerates were detected over this region. Considering the sensitivity of the xrf system is one 2-5nm radius Ni or Cu precipitate at each measured $1\mu m^2$ point, these results show no Ni or Cu exists in this region at a size >2-5nm. Theoretical dissolution modeling indicates that even a $1\mu m$ radius precipitate should fully dissolve with this 800°C-3 hour heat treatment, thus, the precipitates in Figure 2 would be expected to completely dissolve after the gettering treatment. Additionally, this 800°C-3 hour aluminum gettering treatment should be more than sufficient to decrease the Ni and Cu concentration throughout the silicon by many orders of magnitude considering simple diffusion of the impurities from the silicon matrix into the aluminum layer which acts as a near infinite sink. However, by summing the spectra of each point in the xrf scans following aluminum gettering (Figure 3) trace amounts of Ni and Cu were detected as shown in the summed spectra of Figure 4. The Ni Kα peak at 7.45keV is apparent as is the W Lα1 peak

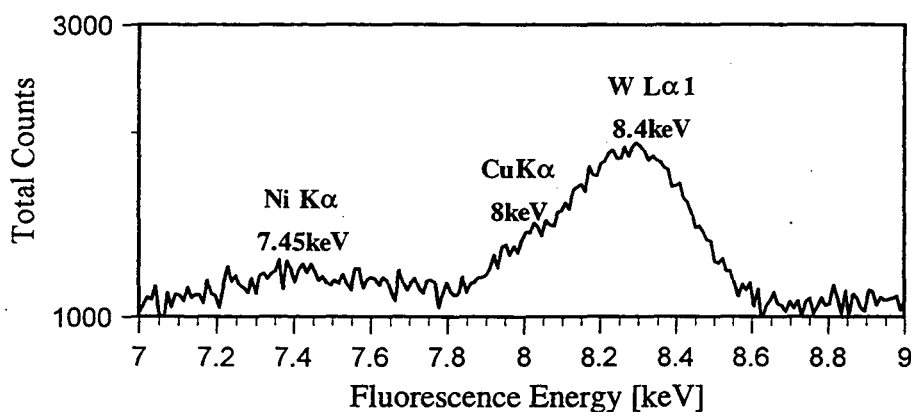
Figure 4: Summed XRF spectra from aluminum gettered sample of Figure 3. Sum taken over 372 points.

at 8.4keV. The W arises from stray radiation off the apparatus and is uniformly distributed across all scan points. The Cu Kα peak at 8keV is washed-out by the WLα1 peak but produces a pronounced tail of the W peak at lower energies which is not present in other materials which are Cu-free. This summed spectra indicates trace amounts of Ni and Cu are present in this region of the sample and the aluminum gettering was unexpectedly incomplete. Based on the fact that Ni and Cu precipitate rapidly in silicon even at room temperature, the Ni and Cu is in the form of precipitates/agglomerates <2-5nm in radii during xrf measurement rather than dissolved in the silicon matrix. However, while at the high temperatures during gettering the Ni and Cu may be in a dissolved form.

The structural defects in the region measured in Figures 1-3 were revealed with preferential etching and microscopy, shown in Figure 5. The lines indicate grain boundaries and the deep, black pits are associated with dislocations. A direct correlation is seen between the Ni and Cu rich regions and dislocations and to a lesser extent grain boundaries. The arrow farthest down and to the right points to a very shallow etch pit which is uncharacteristic for dislocations and grain boundaries. This pit shape is typically related to a microdefect such as a swirl defect, oxygen precipitate, etc.

DISCUSSION AND CONCLUSIONS

Based on the results presented here, the picture of Ni and Cu precipitate dissolution in polysilicon can be described as follows. Impurity precipitates in as-grown polysilicon are found at structural defects, specifically dislocations, to a lesser extent grain boundaries and possibly
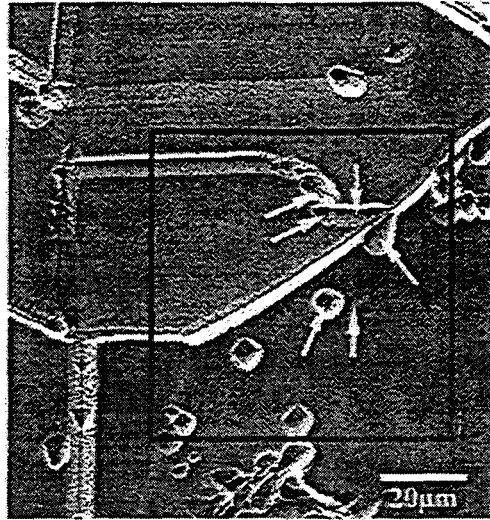
4

Figure 5: Secondary electron image from a Scanning Electron Microscope of the xrf mapped regions of Figures 1-3 after preferential etching. The black box indicates the xrf mapped region from Figure 3 and the white arrows indicate where the Ni and Cu rich regions were in the as-grown material.

microdefects. They readily dissolve when present in moderate to large size >2-5nm, indicating the strain field of defects is not large enough to stabilize a precipitate of this size. Extended gettering treatments dissolve all measurable precipitates (>2-5nm) but leave behind residual Ni and Cu in precipitates <2-5nm in radii. During the gettering heat treatment, the structural defects either act as a region of higher impurity solubility than the surrounding defect-free silicon matrix or the defects stabilize Ni and Cu precipitates of size < 2-5nm. Additionally, the metal impurities may be in the form of metal-oxides or carbides which would completely change the impurity solubility in the surrounding silicon and thus change the gettering kinetics. Some of these concepts are shown graphically by the Gibb's Free Energy for dissolution curve vs. precipitate radius, in Figure 6.
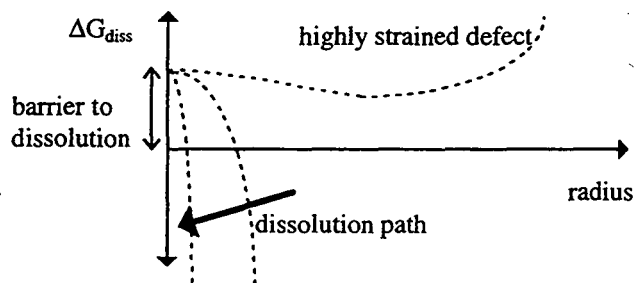

Figure 6: Theoretical Gibb's Free Energy dissolution curve vs. precipitate radius for the case of a precipitate at a highly strained defect and for a precipitate with a barrier to dissolution.

Here we see large precipitates can only survive dissolution if they are stabilized by a highly strained defect which is not experimentally observed in this work. Also, the thermodynamic dissolution path is outlined for the case when a barrier to dissolution exists such that very small precipitates can survive the dissolution process. This barrier may also be considered as residual impurities remaining in the core of the defect where the impurity solubility is significantly higher than the surrounding silicon matrix.

In summation, the release of metal impurities from their previously precipitated state is initially rapid with no apparent barrier. However, complete gettering of the impurities does not

5

occur suggesting either a barrier to release occurs at very small precipitate sizes (<2-5nm) or the impurity is in a dissolved state within the phase of the structural defect.

ACKNOWLEDGMENTS

REFERENCES

[1] C. Cabanel and J.Y. Laval, J. Appl. Phys. **67**, 1425 (1990)

[2] V. Higgs and M. Kittler, Appl. Phys. Lett. **63**, 2085 (1993)

[3] M. Kittler, W. Seifert and V. Higgs, Phys. Stat. Sol. (a) **137**, 327 (1993)

[4] T.S. Fell, P.R. Wilshaw and M.D.d. Coteau, Phys. Stat. Sol. (a) **138**, 695 (1993)

[5] T.H. Wang, T.F. Ciszek and T. Schuyler, Solar Cells **24**, 135 (1988)

[6] S.A. McHugo and W.D. Sawyer, Appl. Phys. Lett. **62**, 2519 (1993)

[7] M. Loghmarti, R. Stuck, J.C. Muller, D. Sayah and P. Siffert, Appl. Phys. Lett., **62**, 979 (1993)

[8] I. Perichaud, F. Floret, M.Stemmer and S. Martinuzzi, Solid State Phen. **32-33**, 77 (1993)

[9] O. Porre, M. Stemmer, M. Pasquinelli, Mat. Sci. & Eng. **B24**, 188 (1994)

[10] B.L. Sopori, L. Jastrzebski, T. Tan, S. Narayanan in *Proc. of the 12th European Photovoltaic Solar Energy Conf.*, Netherlands, 1994, p. 1003

[11] S.A. McHugo, H. Hieslmair, E.R. Weber, Appl. Phys. A **64**, 127 (1997)

[12] M. Seibt, "6th workshop on the role of impurities and defects in silicon device processing", Aug. 12-14, 1996, Snowmass Village, Colorado, to be published

[13] M.Wright-Jenkins, J. Elec. Soc. **124**, 757 (1977)

[14] E.R. Weber, Appl. Phys. A **30**, 1 (1983)

[15] M.J. Whelan, Metal Science Journal **3**, 95 (1969)

[16] H.B. Aaron and G.R. Kotler, Metallurgical Trans. **2**, 392 (1971)